Journal of Electronic Research and Application, 2026, Volume 10, Issue 6
http://ojs.bbwpublisher.com/index.php/JERA
Online ISSN: 2208-3510
Print ISSN: 2208-3502

Finite-Element Modeling and Analytical Validation of a Coaxial Cylindrical Capacitor Using Maxwell 2D

Qi Wang*

School of Electronic and Information Engineering, Liaoning Technical University (Huludao Campus), Huludao 125105, Liaoning, China

***Corresponding author:** Qi Wang, wangqi545@163.com

Abstract: To improve the reliability of capacitance prediction for compact coaxial components, a cylindrical capacitor with copper conductors and an air dielectric is modeled and verified by Ansys Maxwell 2D electrostatic simulation. The inner conductor radius is 0.6 mm, the outer conductor inner radius is 1.0 mm, and the outer conductor wall thickness is 0.2 mm. A 1 V potential is assigned to the inner conductor, while the outer conductor is grounded. Based on Gauss's law, the analytical per-unit-length capacitance is calculated to be 108.9 pF/m. The finite-element model yields 107.4 pF/m, corresponding to a relative error of 1.38%. The simulated electric-field distribution is radially symmetric and reaches its maximum near the inner conductor, which agrees with the theoretical relation $E(r) \propto 1/r$. The results show that Maxwell 2D can accurately reproduce the electrostatic behavior of coaxial capacitors and provide an efficient workflow for capacitance extraction, field visualization, and preliminary structural optimization.

Keywords: Coaxial cylindrical capacitor; Capacitance extraction; Maxwell 2D; Finite-element method; Electric-field distribution

---

1. Introduction

Capacitors are fundamental passive components in electronic systems and are widely used for filtering, coupling, decoupling, energy storage, and signal integrity control [1]. With radio-frequency modules, medical electronics, and compact sensing devices advancing toward miniaturization and high reliability, accurate prediction of capacitance and local electric-field concentration before fabrication is increasingly important [2]. Coaxial cylindrical capacitors are representative structures owing to their compact geometry, uniform field distribution, and direct relationship among capacitance, conductor radius, and dielectric properties [3–5].

Traditional capacitor design often relies on repeated prototyping or empirical adjustment. At the same time, numerical electromagnetic simulation can evaluate capacitance, visualize field concentration, and analyze geometric influence more efficiently at the design stage [6]. For coaxial structures, analytical electrostatic theory provides a clear reference solution [7]. Therefore, comparison between analytical calculations and finite-element simulations is an effective way to verify model accuracy [7–9]. In this study, a copper-air coaxial capacitor is established in Ansys Maxwell 2D. The capacitance and electric-field distribution are extracted from the electrostatic solution, compared with the theoretical value derived from Gauss's law, and discussed in terms of mesh size, boundary representation, and numerical convergence [10].

2. Physical model and analytical formulation

2.1. Coaxial capacitor configuration

The investigated structure consists of two coaxial cylindrical conductors separated by air. The inner solid conductor is used as the high-potential electrode, and the outer annular conductor serves as the grounded shield. The inner conductor radius is a = 0.6 mm, the outer conductor inner radius is b = 1.0 mm, and the outer conductor wall thickness is 0.2 mm. In the two-dimensional electrostatic model, the cross section represents a uniform, infinitely long coaxial structure, so the extracted capacitance is interpreted as per-unit-length capacitance. See **Figure 1**.

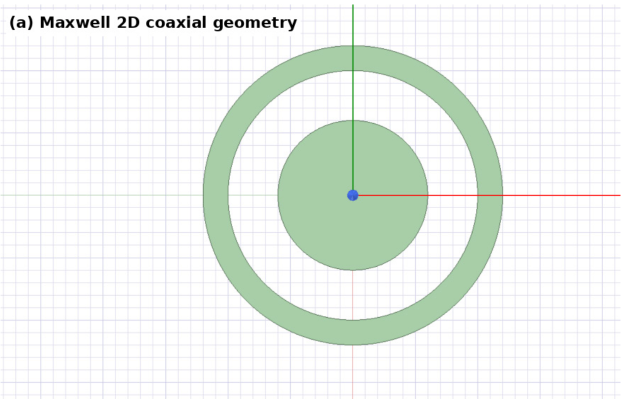

Figure 1. Two-dimensional coaxial capacitor geometry used in the Maxwell electrostatic model.

In the region $a < r < b$ The dielectric is air, and there is no free-volume charge. By applying Gauss's law to a coaxial cylindrical surface, the radial electric field can be expressed as $E(r) = \lambda / (2\pi\varepsilon r)$ where λ is the line charge density and ε is the permittivity of the medium. Integrating the electric field between the two conductors gives the potential difference:

$$U = \int_a^b E(r)\,dr = \frac{\lambda ln(b/a)}{2\pi\varepsilon}$$

Therefore, the per-unit-length capacitance is obtained as:

$$C' = \frac{\lambda}{U} = \frac{2\pi\varepsilon}{ln(b/a)}$$

For air, ε is approximately ε_0. Substituting $a = 0.6\text{mm}$ and $b = 1.0\text{mm}$ gives $ln(b/a) = ln(1.6667) = 0.5108$, *andtheanalyticalresultis* $1.089\times10^{-10}\,F/m$ namely, 108.9pF/m This value serves as the benchmark for validating the Maxwell 2D simulation results. See **Table 1**.

Table 1. Model parameters and theoretical evaluation basis

Item	Value	Role in the model
Inner conductor radius a	0.6 mm	Defines the high-potential central electrode
Outer conductor inner radius b	1.0 mm	Determines the air-gap radius for radial field formation
Outer conductor wall thickness	0.2 mm	Represents the grounded copper shield
Dielectric medium	Air, εr ≈ 1	Stores electrostatic energy between the electrodes
Excitation and boundary	1 V inner; 0 V outer	Forms the electrostatic potential difference
Analytical reference	C’ = 108.9 pF/m	Used to verify the finite-element result

3. Maxwell 2D finite-element simulation method

3.1. Modeling and boundary assignment

The finite-element model is built in Ansys Maxwell 2D under an electrostatic solution type. First, the concentric circular regions are drawn according to the specified radii. Copper is assigned to the inner and outer conductors, and the space between them is set as air. The outer conductor surface is defined as the ground reference at 0 V, and a 1 V excitation is applied to the inner conductor. This boundary setting reproduces the ideal coaxial capacitor condition and enables capacitance extraction from the electrostatic matrix.

After material and excitation assignments, the capacitance matrix is computed using the solver. The simulation focuses on two outputs: the capacitance at the voltage terminal and the spatial distribution of the electric field. The former provides a quantitative index for comparison with theory, whereas the latter gives physical evidence of whether the field is mainly radial and concentrated near the smaller-radius electrode. See **Figure 2**.

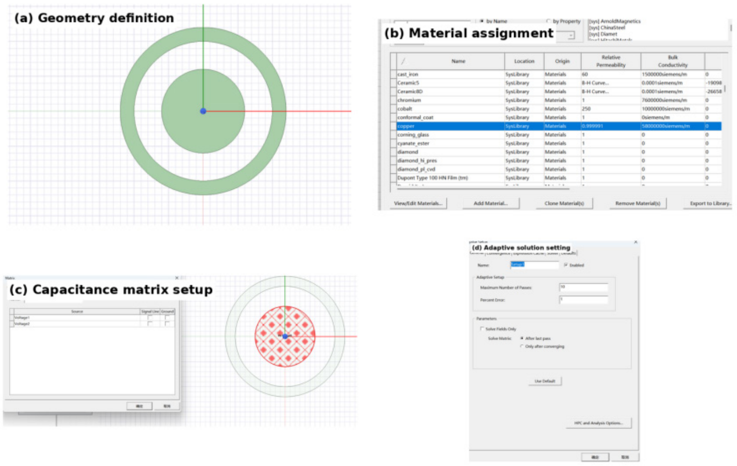

Name	Location	Origin	Relative Permeability	Bulk Conductivity	
cast_iron	SysLibrary	Materials	60	1500000siemens/m	0
Ceramic5	SysLibrary	Materials	B-H Curve...	0.0001siemens/m	-19098
Ceramic8D	SysLibrary	Materials	B-H Curve...	0.0001siemens/m	-26658
chromium	SysLibrary	Materials	1	7600000siemens/m	0
cobalt	SysLibrary	Materials	250	10000000siemens/m	0
conformal_coat	SysLibrary	Materials	1	0siemens/m	0
copper	SysLibrary	Materials	0.999991	58000000siemens/m	0
corning_glass	SysLibrary	Materials	1	0	0
cyanate_ester	SysLibrary	Materials	1	0	0
diamond	SysLibrary	Materials	1	0	0
diamond_hi_pres	SysLibrary	Materials	1	0	0
diamond_pl_cvd	SysLibrary	Materials	1	0	0
Dupont Type 100 HN Film (tm)	SysLibrary	Materials	1	0	0

Name: Setup1 ☑ Enabled

Adaptive Setup

Maximum Number of Passes: 10

Percent Error: 1

Parameters

☐ Solve Fields Only

Solve Matrix: ● After last pass ○ Only after converging

Figure 2. Maxwell 2D modeling procedure: geometry definition, material assignment, capacitance-matrix setup, and adaptive solution setting.

3.2. Numerical evaluation indicators

The relative error between the simulated capacitance and the analytical value is used as the primary validation metric, and an error below 5% is considered acceptable for preliminary engineering evaluation. The electric-field distribution is also examined qualitatively. For a correct coaxial electrostatic solution, the field should be primarily radial, strongest near the inner conductor, and decrease gradually with increasing radius.

Since the numerical solution is obtained on a finite mesh, a slight deviation from the closed-form result is unavoidable. Possible error sources include circular-boundary discretization, finite computational-region treatment, solver residuals, and the ideal assumptions used in the analytical model.

4. Results and discussion

4.1. Capacitance extraction and electric-field distribution

The Maxwell 2D simulation gives a capacitance of 107.4 pF/m. As shown in **Figure 3**, the electric field is mainly radial, starting from the inner conductor and ending on the grounded outer conductor. The field intensity is highest near the inner conductor and decreases outward, which agrees with the theoretical relation E(r) ∝ 1/r. This confirms that the finite-element model accurately describes the electrostatic behavior of the coaxial capacitor.

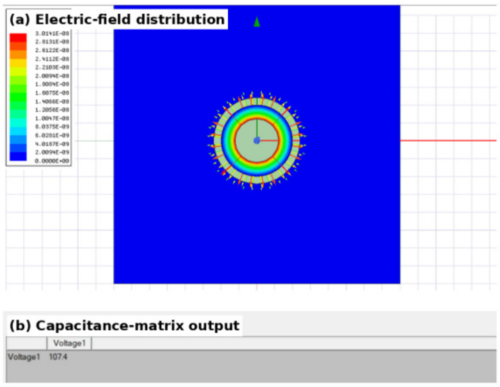

	Voltage1
Voltage1	107.4

Figure 3. Simulation outputs: electric-field distribution and capacitance-matrix result showing 107.4 pF/m.

4.2. Accuracy verification and error analysis

Compared with the analytical reference of 108.9 pF/m, the relative error of the simulation is calculated as

$$\delta = \frac{\left|108.9107.4\right|}{108.9} \times 100\% = 1.38\%$$

The error is well below the 5% design criterion, indicating that the model is sufficiently accurate for the training-stage design and preliminary engineering evaluation. The close agreement also indicates that the adopted cross-sectional model preserves the coaxial symmetry and that the air dielectric has been correctly assigned. See **Table 2**.

Table 2. Comparison between finite-element simulation and analytical calculation

Index	Simulation result	Analytical reference	Evaluation
Capacitance C’	107.4 pF/m	108.9 pF/m	Relative error: 1.38%
Field pattern	Radial distribution: strongest near the inner	$E(r) \propto 1/r$	Consistent with theory
Accuracy requirement	Error below 5%	Design criterion	Satisfied

The remaining difference between theory and simulation is mainly attributable to mesh approximation and numerical truncation. Discrete finite elements represent a circular boundary, so the exact geometry cannot be reproduced without sufficiently fine meshing. In addition, the solver stops after meeting its convergence criterion rather than reaching an exact analytical solution. For higher-precision design, mesh convergence testing, local refinement near conductor edges, and comparison under different boundary extents should be performed.

From an engineering perspective, the verified model can be used for rapid parametric studies. Increasing the dielectric constant would proportionally increase capacitance, while changing the radius ratio b/a would directly alter the logarithmic denominator in the capacitance expression. Therefore, the modeling workflow is suitable for evaluating coupling and decoupling capacitors in high-frequency modules, compact electronic packages, and other structures where electric-field concentration must be controlled.

5. Conclusion

A coaxial cylindrical capacitor with copper conductors and an air dielectric was modeled and analyzed using Ansys Maxwell 2D. The inner conductor radius was 0.6 mm, the outer conductor inner radius was 1.0 mm, and the grounded outer wall thickness was 0.2 mm. With a 1 V excitation applied to the inner conductor, the simulated per-unit-length capacitance was 107.4 pF/m. The theoretical value derived from Gauss law was 108.9 pF/m, yielding a relative error of 1.38%. The electric-field distribution was predominantly radial, and the strongest field occurred near the inner conductor, consistent with electrostatic theory. These results verify the accuracy of the finite-element model and demonstrate that Maxwell 2D is effective for predicting capacitance, visualizing fields, and early-stage optimization of cylindrical capacitor structures. Future work should include mesh convergence tests, dielectric material comparison, finite-length end-effect analysis, and experimental measurements.

Disclosure statement

The author declares no conflict of interest.

References

[1] Osorio L, Hall S, Saavedra R, et al., 2025, Finite Element Modeling for Biophysical Models of Nervous System Stimulation: Best Practices for Multiscale Adaptive Meshing. IEEE Transactions on Neural Systems and Rehabilitation Engineering, 33: 298–309.

[2] Chan M, Chiang K, 2025, Study on the Applicability of Multi-Point Constraints for 3D WLP Finite Element Model. 2025 26th International Conference on Thermal, Mechanical and Multi-Physics Simulation and

Experiments in Microelectronics and Microsystems (EuroSimE), Utrecht, Netherlands: 1–5.

[3] Jiang C, Deng F, Wang Y, et al., 2026, Experimental Verification of Finite Element Modeling for ICT-Type DC High-Voltage Power Supply. IEEE Transactions on Applied Superconductivity, 36(3): 1–6.

[4] Sharma R, Soni P, Mohale V, 2026, Development and Electrical Characterization of Compact High-Voltage Film-Foil Cylindrical Pulse Capacitor. IEEE Transactions on Plasma Science.

[5] Fujita K, Kuramoto N, 2024, Finite-Element Simulations of the Effects of Shielding and Guarding of a Capacitor Using Coaxial Cylindrical Electrodes for Electrostatic Force Balance Measurements. 2024 Conference on Precision Electromagnetic Measurements (CPEM), Denver, USA: 1–2.

[6] Fujita K, Kaneko N, Domae A, et al., 2025, Effects of Shielding and Guarding Electrodes on Electrostatic-Force Balance Measurements in a Coaxial Cylindrical Capacitor. IEEE Transactions on Instrumentation and Measurement, 74: 1–11.

[7] Alavi S, Sumaiya O, Silva D, et al., 2026, Benchmarking Machine Learning Methods Against Finite Element and Empirical Models for Predicting Solder Joint Characteristic Life. IEEE Transactions on Components, Packaging and Manufacturing Technology, 16(5): 1047–1061.

[8] Elkin S, Haider M, Roth T, 2026, Finite-Element Time-Domain Model for Lossy Josephson Traveling-Wave Parametric Amplifiers. IEEE Microwave and Wireless Technology Letters, 36(4): 489–492.

[9] Zhao L, Zhao B, 2026, Co-Simulation and Performance Analysis of Tidal Current Energy PMSG with RMxprt & Maxwell 2D. 2026 6th International Conference on Advances in Electrical, Electronics and Computing Technology (EECT), Hangzhou, China: 1–5.

[10] Zhao Y, Zhang Y, 2025, Frequency Response Function-Based Finite Element Model Updating Using Principal Component Analysis and Extreme Learning Machine. 2025 5th International Conference on Machine Manufacturing and Intelligent Control (ICMMIC), Tianshui, China: 22–25.